ComTech: Computer, Mathematics and Engineering Applications, 16(2), December 2025, 99−115 P-ISSN: 2087-1244
DOI: 10.21512/comtech.v16i2.13000 E-ISSN: 2476-907X

Turning DIN 19682-7 Procedure of Infiltration Rate of Soils Test into the Mobile App for Cloud Storage

Totok Sulistyo[1]*; Mariatul Kiptiah[2]; Sari Bahagiarti Kusumayudha[3]; Tedy Agung Cahyadi[4]; Reza Adhi Fajar[5]

[1]Road and Bridges Construction Engineering Study Program, Civil Engineering Department, Politeknik Negeri Balikpapan, Kalimantan Timur, Indonesia 76129
[1]Doctoral Program in Geological Engineering, Geological Engineering Department, Faculty of Mineral Technology and Energy, Universitas Pembangunan Nasional Veteran Yogyakarta, Yogyakarta, Indonesia 55283
[2]Civil Engineering Study Program, Civil Engineering Department, Politeknik Negeri Balikpapan, Kalimantan Timur, Indonesia 76129
[3]Geological Engineering Department, Faculty of Mineral Technology and Energy, Universitas Pembangunan Nasional Veteran Yogyakarta, Yogyakarta, Indonesia 55283
[4]Mining Engineering Department, Faculty of Mineral Technology and Energy, Universitas Pembangunan Nasional Veteran Yogyakarta, Yogyakarta, Indonesia 55283
[5]Mining Engineering Study Program, Civil Engineering and Earth Science Departement, Politeknik Negeri Banjarmasin, Kalimantan Selatan, Indonesia 70124
[1]totok.sulistyo@poltekba.ac.id; [2]mariatul.kiptiah@poltekba.ac.id; [3]saribk@upnyk.ac.id; [4]tedyagungc@upnyk.ac.id; [5]reza@poliban.ac.id

Received: 2nd February 2025/ **Revised:** 2nd August 2025/ **Accepted:** 4th August 2025

How to Cite: Sulistyo, T., Kiptiah, M., Kusumayudha, S. B., Cahyadi, T. A., & Fajar, R. A. (2025). Turning DIN 19682-7 procedure of infiltration rate of soils test into the mobile app for cloud storage. *ComTech: Computer, Mathematics and Engineering Applications, 16*(2), 99−115. https://doi.org/10.21512/comtech.v16i2.13000

Abstract **-** The in-situ soil infiltration test using a double ring infiltrometer (DRI) apparatus can be conducted in the field according to DIN 19682-7 standards and procedures. As required by these standards, the traditional paper-based measurement form can be replaced with a new application developed to meet standard requirements. The DRI apparatus consists of two concentric rings placed in the soil, filled with water, while the outer ring maintains a constant water level. The water level drop in the inner ring is observed and recorded at regular intervals. The infiltration rate can be calculated for each interval by measuring the change in water height over time. This new application facilitates the automatic calculation of both the actual soil infiltration rate and the Horton soil infiltration model. Comparison tests between the application results and Excel calculations have yielded similar outcomes. The goal of this research is to develop a mobile web-based application for recording data and calculating soil infiltration measurements using the DRI method. The research methodology involves transforming the measurement procedure into a concept, designing the application, and then implementing that design. By replacing the paper-based process, this application will enhance the efficiency, accuracy, and flexibility of soil infiltration measurement projects in various locations. Furthermore, the data will be stored in the cloud, allowing for crowdsourced infiltration data collection and monitoring from any location, including the office.

Keywords**:** soil infiltration, mobile web application, Horton soil infiltration, DIN 19682-7, crowdsourcing, cloud computing

I. INTRODUCTION

The standard method for measuring soil infiltration in the field, known as in situ measurement, involves a surveyor using paper forms to record water drawdown in the ring of a Double-Ring Infiltrometer (DRI) over a specific time interval. However, this traditional method requires modification to reduce systematic errors (Vandervaere et al., 2000). Paper measurement forms are susceptible to damage from rain or sweat, and handwritten notes can vary in legibility and clarity depending on the note-taker's level of fatigue (Sulistyo et al., 2020). When field notes lack clarity, their integrity may be called into question. Therefore, there is a need for innovative technological advancements to replace

*Corresponding Author

the conventional procedure of filling out in situ test forms, minimizing potential human errors. Recent advancements in mobile technology offer a novel and faster approach for recording and storing in situ soil infiltration measurements. This new method will improve data collection and enhance the utilization of the acquired data.

The soil infiltration data obtained can be used for various further analyses, including runoff prediction, flood forecasting, and drainage design. Poor-quality soil infiltration data can lead to significant consequences, such as inaccuracies in flood analysis and mitigation planning. In contrast, high-quality data can be beneficial in fields such as agriculture, hydrology, and environmental engineering (Sun et al., 2024).

One method for assessing soil infiltration is an in situ test using a DRI. The standard measurement procedures for DRI are outlined in DIN 19682-7 and ASTM D3385. These standards detail the methods for determining the infiltration rate of surface water into soil layers using the DRI. The DRI consists of two concentric rings that are inserted into the soil, with water maintained at a constant level within both rings (Abdelmoneim et al., 2021). The infiltration rate is then calculated based on the time taken, the remaining water volume over specific time intervals, and the dimensions of the rings (DIN Media, 2015). Comparatively, the DIN 19682-7 standard offers more straightforward procedures and is primarily used for in situ soil infiltration measurements.

The traditional method for measuring soil infiltration involves recording the initial water height and then introducing water into a DRI setup on the soil. This process has typically been done manually, using either a field book or a paper-based form. However, the growing demand for real-time data has driven the development of field recording systems that leverage ubiquitous and cloud computing (Sulistyo et al., 2022). As a result, soil infiltration data can now be recorded and stored on a cloud server, allowing users to access this information from anywhere at any time.

Moreover, these systems facilitate the rapid recording and collection of simultaneous measurements across vast areas, promoting participatory science or citizen science initiatives (Kouadio et al., 2024). Previous research indicates that data entry via paper-based forms tends to be less accurate, resulting in an error rate of approximately 7%. In contrast, data entry using a personal digital assistant achieves high accuracy, with an error rate of only 1% (Thriemer et al., 2012).

The use of smartphones in soil projects has led to advancements in application development and research within the European Union (EU) countries. This initiative, funded by the EU, aims to enhance existing methodologies and develop new techniques for sensor-based, high-resolution digital soil mapping. The applications have been developed for both Android and iOS platforms, featuring the ability to connect compatible sensors for assessing various soil mapping parameters.

One notable application is “Soilweb," a tool designed for conducting soil surveys. It provides users with access to a database of soil characteristics based on location, including infiltration rates, texture, and water-holding capacity. Experts frequently use this application to gain a deeper understanding of soil properties (Gorthi et al., 2022).

Another study analyzed the use of smartphone cameras as sensors for measuring tension disk infiltrometers using R, yielding results that closely matched those from laboratory experiments (Latorre et al., 2021). Additionally, the smartphone application "LandPKS” was examined, with more information available at https://landpotential.org (Maynard et al., 2022). The accuracy of soil mapping can be validated through decision support system applications, such as LandPKS (Maynard et al., 2023). Further research, utilizing the ABAQUS platform and focusing on expansive soil, reported a reduction in strength due to changes in water content caused by waterfall infiltration (H. Rao et al., 2021). While statistical software has been used to analyze the correlation between soil infiltration rate, texture, and strength, data recording has still been carried out using conventional methods (Cleophas et al., 2022).

This research aims to develop a cloud database for field infiltration data and a dedicated mobile web application, or a responsive web application, based on DIN 19682-7. Soil scientists and hydrologists worldwide use these standards for measuring soil infiltration. The application will allow multiple surveyors to take measurements and record data simultaneously in various locations (Fraisl et al., 2022), with all data stored on a single database server. Other users can retrieve the stored data instantly from the cloud database server using ubiquitous computing. This research suggests that the application reduces the time spent on recording and reporting field infiltration measurements and minimizes potential recording errors due to improved legibility and clarity of field notes. Additionally, the data can be quickly analyzed using the Horton infiltration model, which incorporates the model calculation algorithm within the application.

II. METHODS

The mobile web application designed for recording data from in-situ soil measurements can be operated on any mobile browser platform. The procedures and data requirements are based on the DIN 19682-7 standards. This application will be developed on a cloud web server. It will interact with a database server to perform Create, Retrieve, Update, and Delete (CRUD) operations on data (Negreiros et al., 2023).

The transformation of the DIN 19682-7 standards into the mobile web application involves a series of seven stages. The first stage of this research is a literature review focused on infiltration measurement using DRI, ASTM D3385, and DIN 19682-7. This review aims to provide an understanding

of the latest research and developments in recording methods for in situ infiltration tests. Information gathered from research and review articles published in reputable journals will highlight advancements in technology for measuring in-situ soil infiltration. The process and procedures for conducting in-situ infiltration tests are summarized from best practices outlined in published standards, scientific articles, and books. These resources will inform the design of the application process. The forms and reports generated for in-situ infiltration measurements will primarily adhere to the DIN 19682-7 standards.

The second stage involves designing and implementing database tables in accordance with the standard procedure for in-situ testing. This design takes into account factors such as location conditions, apparatus dimensions, soil type, and the data required during the field test. The process of creating the database is carried out using the phpMyAdmin application on an online server. This includes setting up the CPanel web application, which also installs a web server and a MySQL database server. The resulting database consists of a location table that can store multiple records for each location point, including field measurements. Measurement data will be recorded in the measurement table. Additionally, the application queries the user's table and profile table, temporarily storing this information as session variables when the user logs in (Lala et al., 2021).

The third stage focuses on transforming parameters related to the apparatus, soil, and water—such as the diameter of the ring, soil type, water temperature, initial height, interval time, and differential height—into the user interface. A report template is also provided as a web page, allowing for the display of results from data interpretation and calculations. Key priorities in this user-facing design and implementation stage include flexibility, ergonomics, and user-friendliness (Ding et al., 2025). This stage is accomplished using HTML and CSS.

The fourth stage involves writing PHP code to enhance the user interface's functionality, which includes measurement forms and report templates. This stage also focuses on position marking in the field through location tagging using Google Maps. By utilizing JavaScript and PHP, we can record the geographical coordinates of the measurement location. The geolocation process in this stage leverages webGIS technology based on the Leaflet framework, GeoJSON, and Google Maps to accurately capture the geographical coordinates of the in-situ infiltration measurement location. Once recorded, the location point will be displayed in the webGIS along with its associated attributes (Sergeeva et al., 2022).

The fifth stage encompasses application testing and debugging. This phase ensures that the application functions as expected and helps to identify any bugs or errors. It includes conducting field infiltration tests to discover and correct any mistakes or inaccuracies. Testing is performed for each user interface function of the application by inputting dummy data to verify its functionality. Any errors or malfunctions in the user interface or the application will be addressed and fixed. This thorough testing process is repeated multiple times to ensure that no application bugs remain.

The sixth stage involves verifying that the application complies with DIN 19682-7 standards and specifications. This is done by ensuring that the stored and collected data, time intervals, and calculated infiltration rates align with the DIN 19682-7 standard. The measurement table, calculation results, and report must adhere to both the standard and the requirements outlined in the attachment of DIN 19682-7. To ensure accuracy, the calculation results are verified through manual calculations to confirm that the governing formulas are functioning correctly. The validation process includes comparing the calculation results obtained from the app with those from a spreadsheet calculation. If any noncompliance is identified, it is addressed by revising the calculation algorithm and code, followed by a recheck of the results. This compliance cycle will continue to iterate until the results are aligned with the referenced standards.

The seventh stage focuses on improving the application by incorporating user feedback and requests. Developers aim to enhance both the user interface and functionality in response to user feedback (Cao et al., 2023; Peng, 2024). In this final stage, developers receive user reports that include bug reports on specific features and suggestions for the user interface layout. These insights are acted upon to facilitate ongoing improvements throughout the application's life cycle. Listening to user feedback is essential for refining the application and addressing the evolving needs of users (Bandi et al., 2023). This stage also enables the collection of user data and feedback, which helps identify user needs and opportunities for further application enhancements (Enríquez et al., 2019). Overall, the development process has employed the "divide et impera," or "divide and conquer," approach to translate the initial idea into a functional application. The flow of the development stages is illustrated in Figure 1 (see Appendices).

III. RESULTS AND DISCUSSIONS

The database design was implemented using PHPMyAdmin. The implementation process involved creating, setting up, and modifying the MySQL database's structure. The new database was created by accessing PHPMyAdmin through the CPanel menu provided by the web hosting provider. The next step was to create a database user and password, which were then assigned to the database. These credentials will later be used in the application configuration file to access the CRUD records in each table of the database. The tables created in the database include the users table, user_profile table, location_data table, infiltration_data table, and picture table. An illustration of the table structure and its relationships is shown in Figure 2 (see Appendices).

The user interface design of this application

has been tailored for mobile browsers, prioritizing flexibility, ergonomics, and user-friendliness (Nebe & Heimgärtner, 2024). Figure 3 (see Appendices) presents a use case diagram that illustrates the application's concept and the roles of the various actors involved. This concept is then translated into the user interface design. The application features several user interfaces that allow users to manage their data, including functions for creating, reading, updating, editing, and deleting information. A list of user interfaces designed to meet user needs is presented in Table 1.

Table 1 List of User Interfaces

No	User Interface
1	Login page
2	Register page
3	User profile page
4	Main menu page
5	Plotting location page
6	Form of the measurement data page
7	Editing page
8	Data calculation page
9	Location map page

The main menu page functions as the home page, providing access to all available features, including the user profile, infiltration data, map views of owner data, map views of all user data, and the logout option. This menu appears once the user has completed the authentication process, which includes registering their name and password and completing the login page, as shown in Figure 4 (see Appendices). If the user wishes to return to this page, every feature includes a back button that directs them to the main menu page. The layout of the main menu also serves as the landing page for logged-in users, shown in Figure 5 (see Appendices). Additionally, the application will automatically log the user out after approximately one hour of inactivity.

When the user accesses the infiltration data feature, the browser displays the measurement location page, as shown in Figure 6 (see Appendices). The page also contains the project and data access. The "Add Location" button allows users to add new measurement locations. Clicking this button opens an interactive Google-based map. Users can zoom in or out to pinpoint the exact geographical coordinates of their chosen area. They can refer to various basemap features, such as roads, rivers, buildings, and other landmarks.

A dialog form window will appear on the page, displaying fields for longitude and latitude already filled out, along with empty fields for the location code and remarks. Users can also acquire longitude and latitude data using a geolocation API or smartphone global navigation satellite system (GNSS) sensors (Sulistyo et al., 2025). The base map for location plotting is illustrated in Figure 7 (see Appendices). Once the location data is stored in the database, it will be listed by location names and codes under the "Add Location" button on the Measurement Location page, as depicted in Figure 6 (see Appendices).

The measurement location page can have one or more records of infiltration measurements. If there are no infiltration measurement entries, a red badge will display a zero (0), and the location data will be erasable. Conversely, if there are entries, the total number of measurements will appear on the badge, and the location data will be non-removable. When a location is selected, it will expand to show two option buttons: one for a 5-minute interval infiltration measurement form, and another for an adaptable or flexible interval infiltration measurement form. The list of infiltration measurement data for each location can be edited, displayed, or deleted, as illustrated in Figure 6 (see Appendices).

The infiltration measurement form consists of two pages. The first page is set up for a standard 5-minute interval, while the second page allows for custom interval settings tailored to field conditions or the surveyor's specific needs. These data input forms include fields for time (in seconds), starting height (in centimeters), and ending height (in centimeters). Additionally, these forms feature a stopwatch to provide a time reference for the user when reading the water surface in the inner ring. One of the main advantages of this application is that it eliminates the need for the surveyor to carry various tools for the measurement process. Captured screenshots of these measurement forms are shown in Figure 8 (see Appendices).

The data calculation page displays the infiltration rate table in centimeters per hour (cm/h). This page can also be used to perform advanced calculations for the Horton infiltration rate model, based on the actual infiltration rate. Additionally, it can calculate the trend line from the data regression of time (T) hour and *log(f-fc)*.

The calculation using the Horton model follows several steps. First, the trend line for time versus *log(f-fc)* is represented by the formula in Equation (1). Then, the values of *c* and *m* can be solved using the following Equations (2) and (3). Next, Horton infiltration rate is calculated using Equation (4) (Viessman & Lewis, 2011; Vishwakarma et al., 2024). Where *k* is the intercept and slope of linear regression of *log(f-fc)* against time (Vishwakarma et al., 2024), then the decay constant (*k*) can be solved using the simplified formula in Equation (5).

$$y = mx + c \tag{1}$$

$$c = \frac{\sum y \sum x^2 - \sum x \sum xy}{n \sum x^2 - (\sum x)^2} \tag{2}$$

$$m = \frac{\sum xy - \sum x \sum y}{n \sum x^2 - (\sum x)^2} \tag{3}$$

$$f_t = f_c + (f_o - f_c)e^{-kt} \; for \; 0 \le t \le t_c \tag{4}$$

$$k = \frac{1}{m * 0.434} \quad (5)$$

By selecting the *fc* value from the actual infiltration rate calculation, the application displays the Horton soil infiltration values in the last column of the field measurement data table. The actual infiltration rate and the Horton infiltration rate are then compared. Their results, as defined by Equation (4), are illustrated in Figure 9 (see Appendices).

The final feature is the location map of the measurement point. The location data is converted to GeoJSON format and integrated into the interactive map on OpenStreetMap within the webGIS platform. Information about the data owner and the location name is displayed in a pop-up dialog when the location symbol is selected. This map page is beneficial for monitoring the progress of a soil infiltration measurement project conducted by multiple surveyors across various locations. An illustration of the interactive location map is shown in Figure 10 (see Appendices).

The main coding is performed using native PHP. PHP is essential for implementing the user interfaces and formulas of web-based applications. The code is written to send data to the database and facilitate CRUD operations on the database table. Below are the pseudocodes for the PHP scripts used to calculate the height difference (ΔH) and the time difference (ΔT) on the infiltration measurement form page:

```
variable code = code posted
variable Count
count (variable posted start)
FOR (i=0; i<Count; i++)
variable dh=posted variable end of i – posted
variable start at i
variable hour = posted variable minute at i
variable dt = variable hour at i – variable hour
at (i-1)
variable actual infiltration = variable dh at i /
variable dt at i
IF (variable posted start at i not empty)
SQL Query = INSERT INTO `infiltration_data`
(`data_id`, `project_id`, `t_mnt`, `t_hour`, `h_awal`,
`h_akhir`, `delta_h`, `delta_t`, `dh_per_h` , `uji_
ke`) VALUES (NULL, '"project id at i"', '"minute at
i"', '"hour at i"', '"start at i"', '"end at i"', '"dh at i"',
'"dt at i"', '"infiltration at i"' , '"code"')")
END of IF
END of FOR
```

The list of codes provided will manage the data from soil infiltration tests, encompassing time readings and water drops measured in the inner ring of the DRI. This data is stored in the infiltration_data table within the database, as shown in Figure 11 (see Appendices). The ΔH, ΔT, and the actual infiltration rate generated by the PHP code can be retrieved and displayed as an HTML table, as illustrated in Figure 12 (see Appendices).

The following list of PHP and HTML code display the columns of *fc*, *(f-fc)*, and *log(f-fc)* after the user determines the constant infiltration *(fc)* rate, using the stored variable fc in MySQL. Then, the application conducts the calculations for *(f-fc)* and *log(f-fc)*, and displays the results in the table shown in Figure 12 (see Appendices). The pseudocode for calculating *f-fc* and *log(f-fc)* is provided in Figure 13 (see Appendices) and is also presented below:

```
IF variable fc is selected
        THEN calculate:
        variable f_fc = variable f – variable fc
        variable l_f_fc= log10(variable f_fc)
 END of IF
```

The following code calculates the sums of variables, their squared values, and the squared sums, along with other relevant statistics. These results are essential for conducting linear regression, where time is treated as the *x*-axis and *log(f-fc)* as the *y*-axis. To obtain the summations of *x*, *y*, x^2, and xy each column is processed sequentially. This process is implemented using loop control, as shown in the pseudocode below:

```
variable n = number of row
FOR (variable i = 0; i<n; i++)
        variable Sx+= variable t_hour of i
        variable Sy+=log10(variable f-fc of i)
        variable Sx2+= variable t_hour of i* variable
        t_hour of i
        variable Sxy+= variable t_hour of I *
        log10(variable f-fc of i)
END of FOR

//Variable  Sx = sum of variable t_hour
//Variable Sy =sum of log10 (variable f-fc)
//Varible Sx2 = sum of (variable t_hour *variable
t_hour)
//Variable Sxy = sum of (variable t_hour*
log10(variable f-fc))
```

$$c = \frac{\sum y \sum x^2 - \sum x \sum xy}{n \sum x^2 - (\sum x)^2} \text{ and } m = \frac{\sum xy - \sum x \sum y}{n \sum x^2 - (\sum x)^2} \quad (6)$$

The above code produces a column for each variable along with their sums. These results are then used to derive the linear regression equation $y = mx+c$, where c and m are calculated using Equations (2) and (3), in the following Equation (6). Those Equations can be transformed into the following PHP and HTML code. The values of *c* and *m* are calculated when the code runs. The decay constant *k* can be calculated from Equation (5) where $k = \frac{1}{m * 0.434}$, as depicted in

Figure 14. Pseudocode of calculation of *c*, *m*, and *k* is as follows:

```
variable c = ((variable Sy * variable Sx2)-(variable
             Sx * variable Sxy))/((variable Sx2)-
             (variable Sx * variableSx));
```

variable m = ((variable Sxy)-(variable Sx * variable Sy))/((variable Sx2)-(variable Sx * variable Sx))
variable k = -1/(variable m * 0.434)

$$f_t = f_c + (f_o - f_c)e^{-kt} \quad (7)$$

Equation (7) presents the implementation of the Horton infiltration rate calculation based on Equation (4). An example of the calculation results is illustrated in Figure 15 (see Appendices). The potential benefits of adopting the proposed application can be evaluated by comparing the advantages and disadvantages of recording soil infiltration tests and calculating soil infiltration rates using traditional paper-based forms versus the proposed application. Currently, the DRI in-situ soil infiltration measurement data is typically recorded on a paper form, which can be printed from the DRI apparatus manual. Table 2 presents a comparison between the proposed web-based application and the paper-based method. This comparison highlights the potential benefits of using the proposed application for conducting field measurements of soil infiltration with DRI, as opposed to the conventional paper-based approach.

Table 2 The Strength Comparison of the Paper-based Form and the Proposed Application

Strenghts	Paper-based	Web-based
Error-prone	+	-
Greater Data sharing and accessibility	-	+
Automatomation Feature	-	+
Faster (less time)	-	+
User familiarity (relatively no need for skill)	+	-
Searchability	-	+
Accuracy	-	+
No Power/Electricity/Battery	+	-
No physical storage & protection	-	+
Weather proof	-	+
Eco Friendly	-	+
No dependency	+	-
No need for further work (retype)	-	+
Clarity, Legibility, Tidiness	-	+

The shift to the proposed application is timely, given that most people now use smartphones with internet browsers and can easily access the internet through GSM networks, Wi-Fi, and other means. Another advantage of the proposed application is its potential to facilitate crowdsourcing or citizen science approaches in soil infiltration data collection across larger areas, involving multiple experts in this field (Arienzo et al., 2021; Pudifoot et al., 2021). Furthermore, users can obtain updated data more quickly and cost-effectively for purposes such as research, planning, and predictions.

The developer can enhance the application based on user requirements and feedback. This approach will ultimately benefit the application, making the data more comprehensive and accurate. Users will be able to download more data, resulting in a denser location database that enables faster and more effective work. The stored data can be utilized in various research areas, including flood management, agriculture, groundwater management, drainage, and drought mitigation, among others.

The application can be further developed to meet the specific needs of various users, including researchers, planners, surveyors, students, and teachers, each with their roles and access rights. Additionally, the sensors can be improved to enable automation, which will reduce the tasks surveyors need to perform in the field and increase the accuracy of the uploaded data (A.S. Rao et al., 2022). With advancements in artificial intelligence, the recorded soil infiltration data on the server can be queried by a machine-learning algorithm to predict the soil infiltration rate based on the available stored parameters (Lupián-Machuca et al., 2024; Sulistyo & Fauzi, 2023).

The application is designed for mobile web usage and runs on any mobile platform, including Android, iOS, and Windows phones. As it operates on mobile and internet browsers, installation is not required. However, a limitation of this app is that it cannot directly read geographic coordinates from the built-in GPS for location tagging, as it relies on a server application that is not installed on the smartphone. Instead, the application uses Google Maps to mark and plot the location by pinpointing the area on the map. The advantage of plotting locations using a zoomed-in Google Map is that it provides more accurate coordinates, mainly when the location includes map features such as roads, buildings, rivers, and other landmarks, rather than relying solely on built-in GPS. The plotting of static positions at 10-minute intervals using a smartphone's standard built-in GPS can deviate by 1 to 5 meters from the actual ground truth (Uradziński & Bakuła, 2020).

In comparison with existing products, such as sensor-based infiltrometers that measure soil infiltration rates and automatically transmit data to a cloud server (Whenua, 2019), the proposed application provides a more cost-efficient alternative. It can be used without licensing fees and is compatible with conventional DRI apparatuses. Conversely, commercial products are typically integrated with proprietary infiltrometer devices and sensor systems.

IV. CONCLUSIONS

The developed application is designed for recording and calculating soil infiltration using the DRI method, following the DIN 19682-7 procedure.

This method has demonstrated its effectiveness by automating data calculations, which reduces the time needed for the data cycle and simplifies automated reporting. Additionally, the proposed application and method enhance data accuracy by minimizing errors associated with illegible handwritten notes, enabling faster calculation of infiltration values from input data compared to previous methods. The function code used in the application produces results that are consistent with those obtained from spreadsheet formulas, enabling calculations to be directly applied in the field once testing is complete. Another significant advantage is enhanced data management, which streamlines the organization, storage, and sharing of test results.

The conversion of DIN 19682-7 into a mobile application presents a significant advancement for professionals in fields such as hydrology, civil engineering, environmental science, and agriculture. This application enables users to conduct infiltration rate tests using the DRI more efficiently, while ensuring adherence to established standardized methods. Multiple groups can perform data measurements concurrently or utilize crowdsourcing techniques, with the capacity to monitor activities remotely. Data can be accessed and reviewed via a cloud server, facilitating streamlined operations and enhanced data management.

The proposed application addresses many limitations of traditional paper-based methods. While it has some drawbacks, such as reliance on electricity, batteries, and internet connectivity in the field, recent advancements in information and communication technology (ICT), cellular technology, and battery technology can help mitigate these challenges. Additionally, a paper-based method can be kept as a backup in case measurements need to be taken in an area with no cellular signal.

The limitations of this application are identified as follows. First, it relies on an internet connection, making it unusable in areas without such access. Second, the built-in GPS cannot determine the user's location; instead, the location must be identified using a map. Nevertheless, the implications of this research suggest that it will gradually replace traditional paper-based recording and calculation procedures for DRI measurements, as well as improve supervision of DRI measurement projects in the near future. In subsequent research, this outcome can be integrated with IoT and sensor technologies to develop autonomous systems for reading and reporting DRI measurements. As a result, human operators will no longer be required to input data.

AUTHOR CONTRIBUTIONS

Conceived and designed the analysis, T. S., T. A. C. and R. A. F.; Collected the data, T. S. and M. K.; Contributed data or analysis tools, T. S., S. B. K. and R. A. F.; Performed the analysis, T. S., S. B. K. and R. A. F.; Wrote the paper, T. S. and M. K.; and Article review, T. A. C. and R. A. F.

DATA AVAILABILITY

The data that support the findings of this study are available from the corresponding author, **[TS]**, upon reasonable request. Explain the reason why the readers must request the data.

ACKNOWLEDGEMENT

Special gratitude goes to the Management of Balikpapan State Polytechnics, which has permitted the use of laboratory facilities.

REFERENCES

Abdelmoneim, A. A., Daccache, A., Khadra, R., Bhanot, M., & Dragonetti, G. (2021). Internet of Things (IoT) for double ring infiltrometer automation. *Computers and Electronics in Agriculture*, *188*, 106324. https://doi.org/10.1016/J.COMPAG.2021.106324

Arienzo, M. M., Collins, M., & Jennings, K. S. (2021). Enhancing Engagement of Citizen Scientists to Monitor Precipitation Phase. *Frontiers in Earth Science*, *9*, 617594. https://doi.org/10.3389/feart.2021.617594

Bandi, A., Adapa, P. V. S. R., & Kuchi, Y. E. V. P. K. (2023). The power of generative ai: A review of requirements, models, input–output formats, evaluation metrics, and challenges. *Future Internet*, *15*(8), 260. https://doi.org/10.3390/FI15080260

Cao, J., Lam, K. Y., Lee, L. H., Liu, X., Hui, P., & Su, X. (2023). Mobile Augmented Reality: User Interfaces, Frameworks, and Intelligence. *ACM Computing Surveys*, *55*(9), 189.

Cleophas, F., Isidore, F., Musta, B., Mohd Ali, B. N., Mahali, M., Zahari, N. Z., & Bidin, K. (2022). Effect of soil physical properties on soil infiltration rates. *Journal of Physics: Conference Series*, *2314*(1), 012020. https://doi.org/10.1088/1742-6596/2314/1/012020

DIN Media. (2015). *DIN 19682-7 - 2015-08*. https://www.dinmedia.de/en/standard/din-19682-7/236310867

Ding, W., Lin, X., & Zarro, M. (2025). *Information Architecture and UX Design.* Springer International Publishing AG. https://doi.org/10.1007/978-3-031-72138-0

Enríquez, J. G., Sánchez-Begines, J. M., Domínguez-Mayo, F. J., García-García, J. A., & Escalona, M. J. (2019). An approach to characterize and evaluate the quality of Product Lifecycle Management Software Systems. *Computer Standards & Interfaces*, *61*, 77–88. https://doi.org/10.1016/J.CSI.2018.05.003

Fraisl, D., Hager, G., Bedessem, B., Gold, M., Hsing, P. Y., Danielsen, F., Hitchcock, C. B., Hulbert, J. M., Piera, J., Spiers, H., Thiel, M., & Haklay, M. (2022). Citizen science in environmental and ecological sciences. *Nature Reviews Methods Primers 2022*, *2*(1), 1–20. https://doi.org/10.1038/s43586-022-00144-4

Gorthi, S., Singh, R., Chakraborty, S., Li, B., & Weindorf, D. C. (2022). Identification of Köppen climate classification and major land resource area in the United States using a smartphone application. *Geoderma Regional*, *30*, 567. https://doi.org/10.1016/j.geodrs.2022.e00567

Whenua, M. (2019). *Cloud-connected, smartphone-driven infiltrometer network*. https://www.landcareresearch.co.nz/publications/soil-horizons/soil-horizons-articles/infiltrometer-network

Kouadio, J. S., Rodriguez, F., Grandvaux, E., & Waksberg, A. (2024). Pathway to design a multiparameter application for environmental monitoring to contribute to citizen well-being. *Nature-Based Solutions*, *5*, 100117. https://doi.org/10.1016/J.NBSJ.2024.100117

Lala, S. K., Kumar, A., & Subbulakshmi, T. (2021). Secure web development using OWASP guidelines. *Proceedings - 5th International Conference on Intelligent Computing and Control Systems, ICICCS 2021*, 323–332. https://doi.org/10.1109/ICICCS51141.2021.9432179

Latorre, B., Moret-Fernández, D., Lyons, M. N., & Palacio, S. (2021). Smartphone-based tension disc infiltrometer for soil hydraulic characterisation. *Journal of Hydrology*, *600*, 126551. https://doi.org/https://doi.org/10.1016/j.jhydrol.2021.126551

Lupián-Machuca, M. R., Cruz-Cárdenas, G., Flores-Magallón, R., Silva-García, J. T., Ochoa-Estrada, S., & Martínez-Trinidad, S. (2024). Prediction of Water Infiltration of Three Types of Soil with Machine Learning in the Sahuayo River Basin. *Applied and Environmental Soil Science*, *2024*(1), 5555105. https://doi.org/10.1155/2024/5555105

Maynard, J. J., Maniak, S., Hamrick, L., Peacock, G., McCord, S. E., & Herrick, J. E. (2022). LandPKS Toolbox: Open-source mobile app tools for sustainable land management. *Journal of Soil and Water Conservation*, *77*(6), 91A-97A.

Maynard, J. J., Yeboah, E., Owusu, S., Buenemann, M., Neff, J. C., & Herrick, J. E. (2023). Accuracy of regional-to-global soil maps for on-farm decision-making: Are soil maps "good enough"? *SOIL*, *9*(1), 277–300. https://doi.org/10.5194/soil-9-277-2023

Nebe, K., & Heimgärtner, R. (2024). Ergonomic Principles in Designing Assistive Systems. In *International Conference on Human-Computer Interaction* (pp. 75-87). https://doi.org/10.1007/978-3-031-60875-9_6

Negreiros, B., Schwindt, S., Scolari, F., Barros, R., Galdos, A. A., Noack, M., Haun, S., & Wieprecht, S. (2023). A database application framework toward data-driven vertical connectivity analysis of rivers. *Environmental Modelling & Software*, *172*, 105916. https://doi.org/10.1016/j.envsoft.2023.105916

Peng, S. (2024). The influence of Graphical User Interfaces on human-computer interaction and the impact of organizing software on decision-making process. *Applied and Computational Engineering*, *50*(1), 213–221. https://doi.org/10.54254/2755-2721/50/20241509

Pudifoot, B., Cárdenas, M. L., Buytaert, W., Paul, J. D., Narraway, C. L., & Loiselle, S. (2021). When it rains, it pours: Integrating citizen science methods to understand resilience of urban green spaces. *Frontiers in Water*, *3*, 654493. https://doi.org/10.3389/FRWA.2021.654493/BIBTEX

Rao, A. S., Radanovic, M., Liu, Y., Hu, S., Fang, Y., Khoshelham, K., Palaniswami, M., & Ngo, T. (2022). Real-time monitoring of construction sites: Sensors, methods, and applications. *Automation in Construction*, *136*, 104099. https://doi.org/10.1016/J.AUTCON.2021.104099

Rao, H., Wang, J., Zhao, Z., Wu, G., & Feng, T. (2021). An analysis of rainfall infiltration of expansive soil slope based on the finite element software custom constitutive model. *Hydrogeology and Engineering Geology*, *48*(1), 154–162. https://doi.org/10.16030/j.cnki.issn.1000-3665.202002020

Sergeeva, J., Filatova, A., Kovalchuk, M., & Teryoshkin, S. (2022). SemAGR: semantic method for accurate geolocations reconstruction within extensive urban sites. *Procedia Computer Science*, *212*, 409–417. https://doi.org/10.1016/J.PROCS.2022.11.025

Sulistyo, T., Achmad, K., & Purnama, I. B. I. (2022). The asset management and tracking system for Technical and Vocational Education and Training (TVET) institution based on ubiquitous computing. *ComTech: Computer, Mathematics and Engineering Applications*, *13*(1), 23–34. https://doi.org/10.21512/COMTECH.V13I1.7342

Sulistyo, T., Achmad, K., & Respati, S. (2020). GeomatikaDroid: An Android application for improving theodolite measurement. *Journal of Physics: Conference Series*, *1450*(1). https://doi.org/10.1088/1742-6596/1450/1/012021

Sulistyo, T., & Fauzi, R. (2023). Soil infiltration rate prediction using machine learning regression model: A case study on Sepinggan River Basin, Balikpapan, Indonesia. *Indonesian Journal on Geoscience*, *10*(3), 335–347. https://doi.org/10.17014/IJOG.10.3.335-347

Sulistyo, T., Kusumayudha, S. B., Cahyadi, T. A., & Fajar, R. A. (2025). Mobile and web-based application as a tool for flood data collection based on citizen science. *Earth Science Informatics 2024, 18*(2), 1–14. https://doi.org/10.1007/S12145-024-01664-1

Sun, C., Tang, C. S., Vahedifard, F., Cheng, Q., Dong, A., Gao, T. F., & Shi, B. (2024). High-resolution monitoring of soil infiltration using distributed fiber optic. *Journal of Hydrology*, *640*, 131691. https://doi.org/10.1016/J.JHYDROL.2024.131691

Thriemer, K., Ley, B., Ame, S. M., Puri, M. K., Hashim, R., Chang, N. Y., Salim, L. A., Ochiai, R. L., Wierzba, T. F., Clemens, J. D., Von Seidlein, L., Deen, J. L., Ali, S. M., & Ali, M. (2012). Replacing paper

data collection forms with electronic data entry in the field: Findings from a study of community-acquired bloodstream infections in Pemba, Zanzibar. *BMC Research Notes*, *5*(1), 1–7. https://doi.org/10.1186/1756-0500-5-113/TABLES/2

Uradziński, M., & Bakuła, M. (2020). Assessment of static positioning accuracy using low-cost smartphone GPS devices for geodetic survey points' determination and monitoring. *Applied Sciences*, *10*(15), 5308. https://doi.org/10.3390/APP10155308

Vandervaere, J.-P., Vauclin, M., & Elrick, D. E. (2000). Transient flow from tension Infiltrometers I. The two-parameter equation. *Soil Science Society of America Journal*, *64*(4), 1263–1272. https://doi.org/10.2136/SSSAJ2000.6441263X

Viessman, W., & Lewis, G. L. (2011). *Introduction to hydrology*. Pearson Education.

Vishwakarma, D. K., Yadav, D., Kumar, R., Kumar, R., Bhat, S. A., Mirzania, E., & Kuriqi, A. (2024). Assessing the performance of various infiltration models to improve water management practices. *Paddy and Water Environment*, 1–17.

APPENDICES

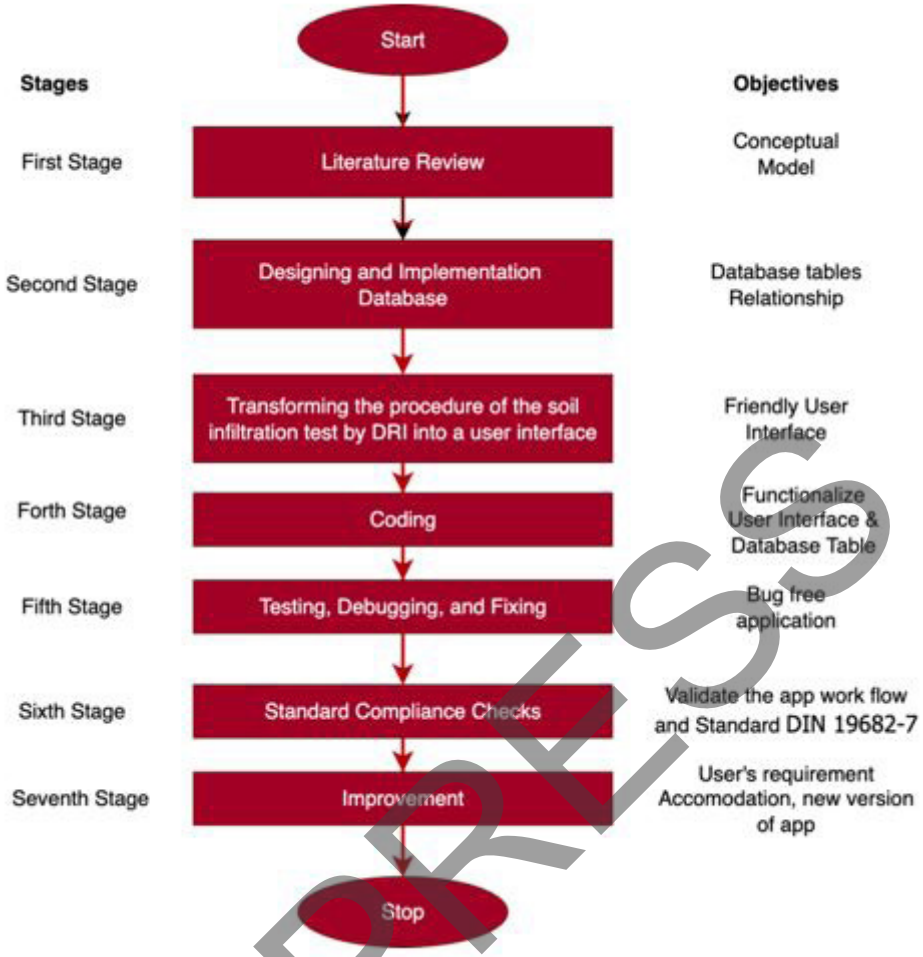

Figure 1 Application Development Stage Flow

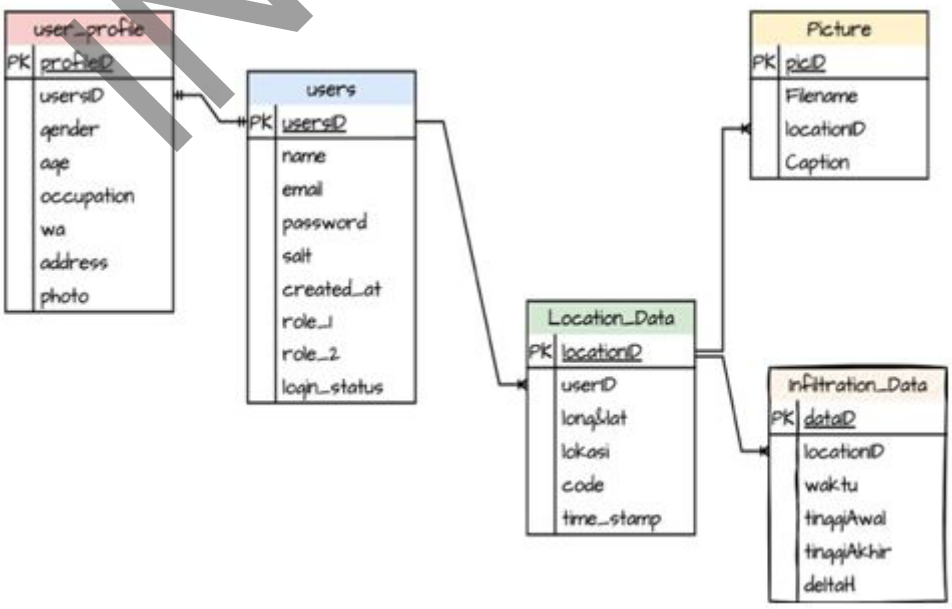

Figure 2 Structure and Relation Design Database Table

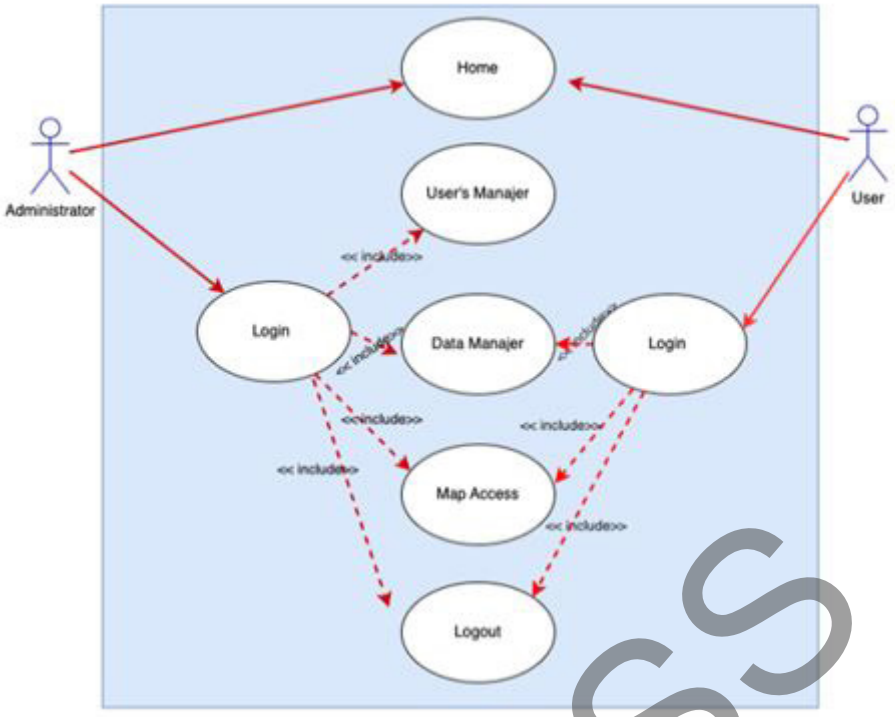

Figure 3 Mobile Web Application Use Case Diagram

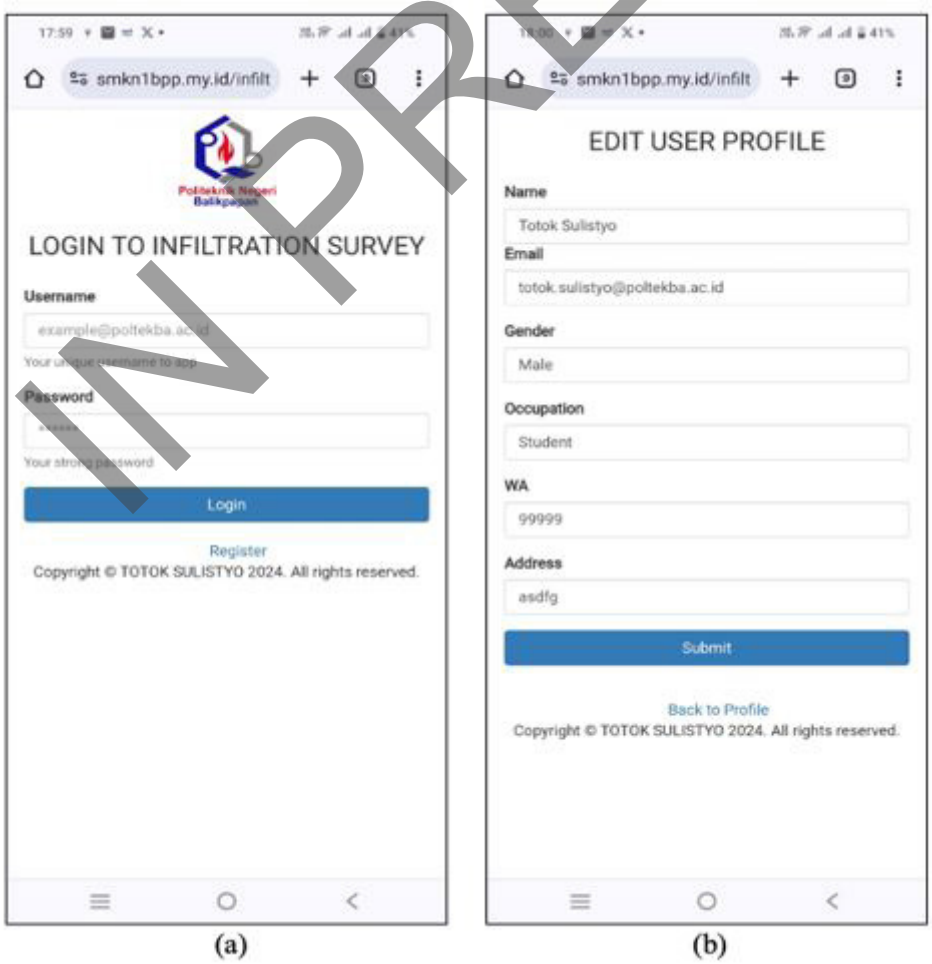

Figure 4 (a) Login Page, (b) User's Profile Page

Figure 5 The Main Menu Page Display

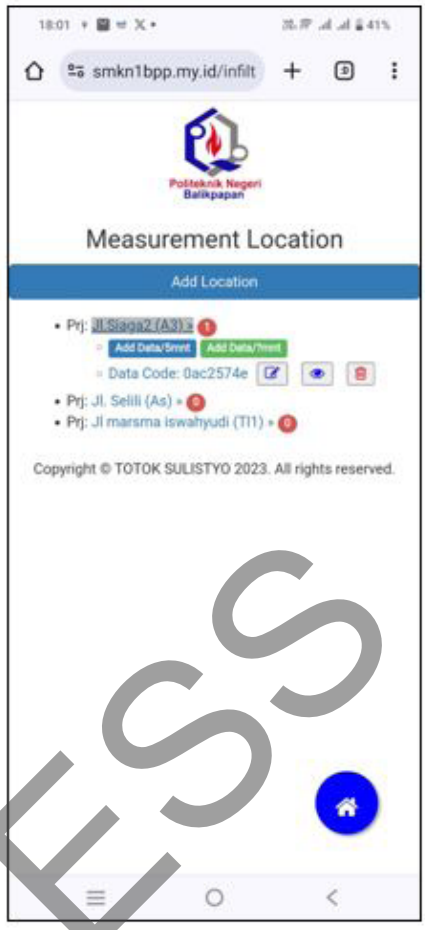

Figure 6 The Measurement Location Page

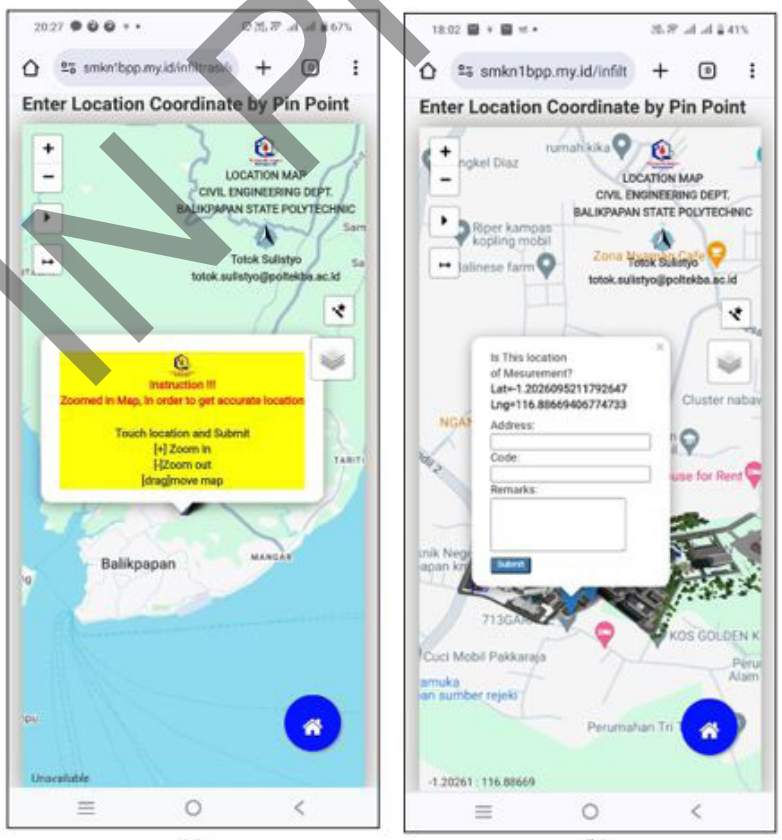

(a) (b)

Figure 7 a) The Plotting Location Map, (b) The Pop-Up Location Form

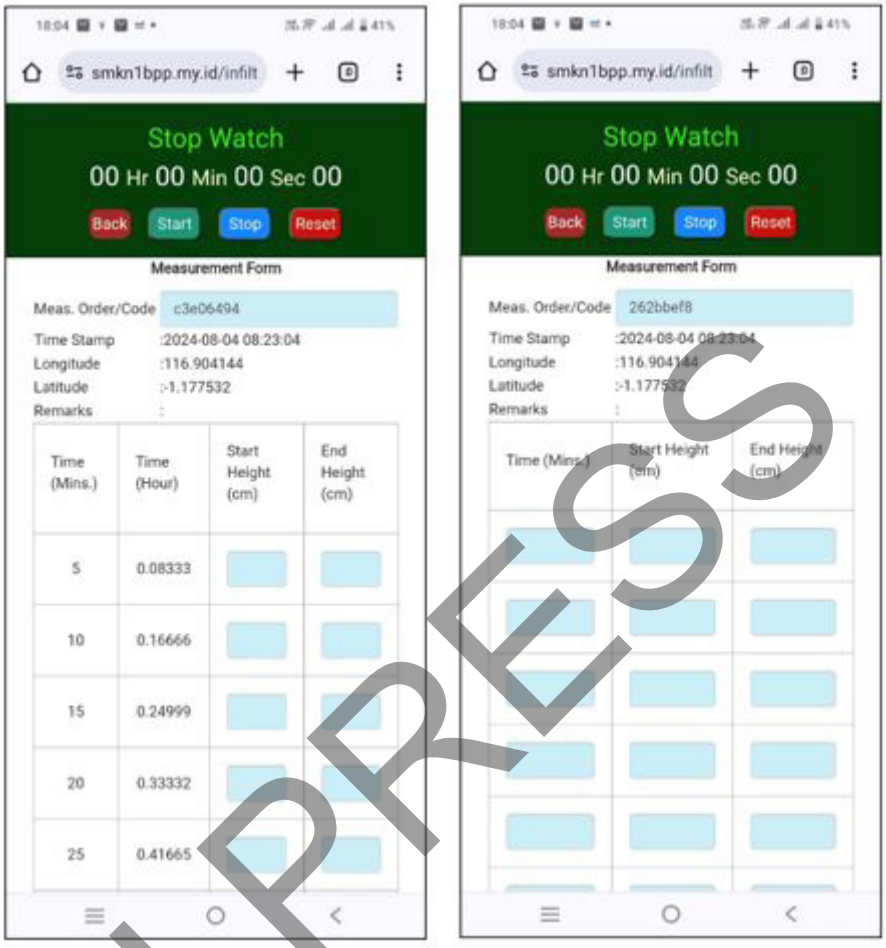

Figure 8 a) Default 5-Minute Interval Form, b) User Setting Interval Form

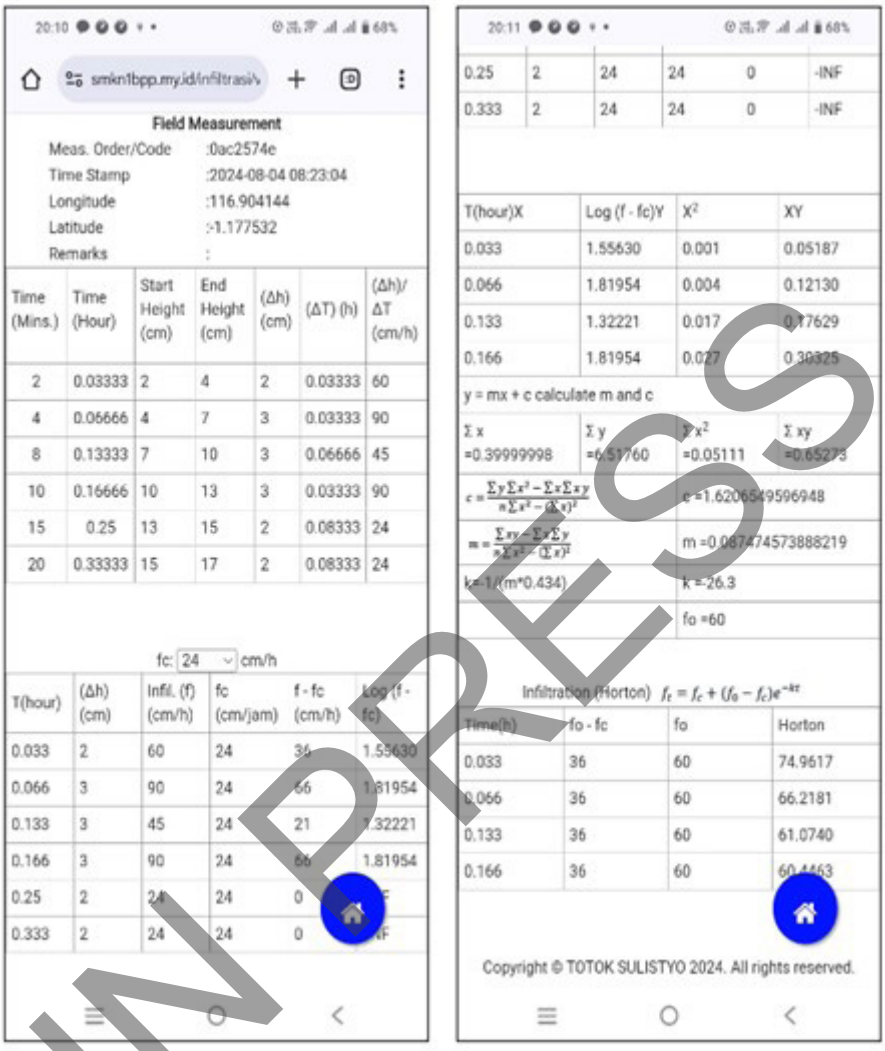

Field Measurement

Meas. Order/Code :0ac2574e
Time Stamp :2024-08-04 08:23:04
Longitude :116.904144
Latitude :-1.177532
Remarks :

Time (Mins.)	Time (Hour)	Start Height (cm)	End Height (cm)	(Δh) (cm)	(ΔT) (h)	(Δh)/ ΔT (cm/h)
2	0.03333	2	4	2	0.03333	60
4	0.06666	4	7	3	0.03333	90
8	0.13333	7	10	3	0.06666	45
10	0.16666	10	13	3	0.03333	90
15	0.25	13	15	2	0.08333	24
20	0.33333	15	17	2	0.08333	24

fc: 24 cm/h

T(hour)	(Δh) (cm)	Infil. (f) (cm/h)	fc (cm/jam)	f - fc (cm/h)	Log (f - fc)
0.033	2	60	24	36	1.55630
0.066	3	90	24	66	1.81954
0.133	3	45	24	21	1.32221
0.166	3	90	24	66	1.81954
0.25	2	24	24	0	-INF
0.333	2	24	24	0	-INF

T(hour)X	Log (f - fc)Y	X^2	XY
0.033	1.55630	0.001	0.05187
0.066	1.81954	0.004	0.12130
0.133	1.32221	0.017	0.17629
0.166	1.81954	0.027	0.30325

y = mx + c calculate m and c

Σ x	Σ y	Σx^2	Σ xy
=0.39999998	=6.51760	=0.05111	=0.65273

$c = \frac{\Sigma y \Sigma x^2 - \Sigma x \Sigma xy}{n\Sigma x^2 - (\Sigma x)^2}$ c =1.6206549596948

$m = \frac{\Sigma xy - \Sigma x \Sigma y}{n\Sigma x^2 - (\Sigma x)^2}$ m =0.087474573888219

k=-1/(m*0.434) k =-26.3

fo =60

Infiltration (Horton) $f_t = f_c + (f_0 - f_c)e^{-kt}$

Time(h)	fo - fc	fo	Horton
0.033	36	60	74.9617
0.066	36	60	66.2181
0.133	36	60	61.0740
0.166	36	60	60.4463

(a) (b)

Figure 9 a) The Measurement Data and Calculated Actual Infiltration Rate,
b) The Calculated Horton Infiltration Rate.

Figure 10 Interactive Location Map.

Showing rows 0 - 6 (7 total, Query took 0.0003 seconds.)

SELECT * FROM `inf_data`

Profiling [Edit inline] [Edit] [Explain SQL] [Create PHP code] [Refresh]

Show all | Number of rows: 25 Filter rows: Search this table Sort by key: None

Extra options

	data_id	project_id	t_mnt	t_hour	h_awal	h_akhir	delta_h	delta_t	dh_per_h	uji_ke
Edit Copy Delete	121	3	2	0.03333333	2	4	2	0.03333333	60	0ac2574e
Edit Copy Delete	122	3	4	0.06666666	4	7	3	0.03333333	90	0ac2574e
Edit Copy Delete	123	3	8	0.13333333	7	10	3	0.06666666	45	0ac2574e
Edit Copy Delete	124	3	10	0.16666666	10	13	3	0.03333333	90	0ac2574e
Edit Copy Delete	125	3	15	0.25	13	15	2	0.08333333	24	0ac2574e
Edit Copy Delete	126	3	20	0.33333333	15	17	2	0.08333333	24	0ac2574e

Check all With selected: Edit Copy Delete Export

Show all | Number of rows: 25 Filter rows: Search this table Sort by key: None

Figure 11 Database table resulted from the posting of infiltration data

Field Measurement

Meas. Order/Code :0ac2574e
Time Stamp :2024-08-04 08:23:04
Longitude :116.904144
Latitude :-1.177532
Remarks :

Time (Mins.)	Time (Hour)	Start Height (cm)	End Height (cm)	(Δh) (cm)	(ΔT) (h)	(Δh)/ΔT (cm/h)
2	0.03333	2	4	2	0.03333	60
4	0.06666	4	7	3	0.03333	90
8	0.13333	7	10	3	0.06666	45
10	0.16666	10	13	3	0.03333	90
15	0.25	13	15	2	0.08333	24
20	0.33333	15	17	2	0.08333	24

Figure 12 H and ΔT Measurement and Calculation Result

fc: 24 cm/h

T(hour)	(Δh) (cm)	Infil. (f) (cm/h)	fc (cm/jam)	f - fc (cm/h)	Log (f - fc)
0.033	2	60	24	36	1.55630
0.066	3	90	24	66	1.81954
0.133	3	45	24	21	1.32221
0.166	3	90	24	66	1.81954

Figure 13 *f – fc* and *log(f-fc)* Calculation Result

T(hour)X	Log (f - fc)Y	X^2	XY
0.033	1.55630	0.001	0.05187
0.066	1.81954	0.004	0.12130
0.133	1.32221	0.017	0.17629
0.166	1.81954	0.027	0.30325
y = mx + c calculate m and c			
Σ x =0.39999998	Σ y =6.51760	Σ x^2 =0.05111	Σ xy =0.65273
$c = \frac{\Sigma y \Sigma x^2 - \Sigma x \Sigma xy}{n\Sigma x^2 - (\Sigma x)^2}$		c =1.6206549596948	
$m = \frac{\Sigma xy - \Sigma x \Sigma y}{n\Sigma x^2 - (\Sigma x)^2}$		m =0.087474573888219	
k=-1/(m*0.434)		k =-26.3	
		fo =60	

Figure 14 The Calculation of *c*, *m*, and *k*

Infiltration (Horton) $f_t = f_c + (f_0 - f_c)e^{-kt}$			
Time(h)	fo - fc	fo	Horton
0.033	36	60	74.9617
0.066	36	60	66.2181
0.133	36	60	61.0740
0.166	36	60	60.4463

Figure 15 The Calculation Results